

## Effect of hadronic rescattering on the elliptic flow after the hydrodynamics model

Guo-Liang Ma,  
Yu-Gang Ma,  
Ben-Hao Sa,  
Xiang-Zhou Cai,  
Ze-Jun He,  
Huang-Zhong Huang,  
Jia-Li Long,  
Wen-Qin Shen,  
Chen Zhong,  
Jin-Hui Chen,  
Jia-Xu Zuo,  
Song Zhang,  
Xing-Hua Shi

**Abstract** A hydrodynamics + hadronic rescattering model is used to simulate Au+Au collisions at 200 GeV and a Cooper-Frye method is adopted for hadronization. The effect of hadronic rescattering on elliptic flow  $V_2$  in 20–40% Au+Au collisions at 200 GeV has been investigated. It is found that the hadronic rescattering can suppress elliptic flow  $V_2$  and makes an asymmetric system in momentum space tend to be less anisotropic. The suppression effect becomes weak with increasing transverse momentum. In addition, the effect of hadronic rescattering on transverse momentum spectra and anisotropy of hadronic coordinate space is presented.

**Key words** elliptic flow • hydrodynamic model • hadronic rescattering • LUCIAE model

G. L. Ma<sup>✉</sup>, X. Z. Cai, J. L. Long, C. Zhong, J. H. Chen,  
J. X. Zuo, S. Zhang, X. H. Shi  
Shanghai Institute of Applied Physics,  
Chinese Academy of Sciences,  
P. O. Box 800-204, Shanghai 201 800, China,  
Tel.: 86-21-59553021, Fax: 86-21-59554781,  
E-mail: glma@sinap.ac.cn

Y. G. Ma, Z. J. He, W. Q. Shen  
Shanghai Institute of Applied Physics,  
Chinese Academy of Sciences,  
P. O. Box 800-204, Shanghai 201800, China  
and China Center of Advanced Sciences and Technology  
(World Laboratory),  
P. O. Box 8730, Beijing 100 080, China

B. H. Sa  
China Institute of Atomic Energy,  
P. O. Box 918, Beijing 102 413, China

H. Z. Huang  
University of California,  
Los Angeles, CA 90095, USA

Received: 30 September 2005  
Accepted: 8 May 2006

Lattice QCD calculations have predicted a transition from quark-gluon matter (QGP) to hadronic matter at high temperature or density [23, 24]. This phase transition is believed to occur around ten microseconds after Big Bang. Practically, one may obtain this piece of information by studying the relativistic heavy-ion collisions at Brookhaven National Laboratory now. Some possible probes have been proposed for searching for it [10, 20]. Elliptic flow  $V_2$  is one of these probes, from which one may understand the information on the early state in relativistic heavy-ion collisions through measuring anisotropy of momentum space of particles in final state. Some experimental results from BNL-RHIC have been published recently [1–7].

As we know, hydrodynamical model, which is one method to study relativistic heavy-ion collisions, can reproduce convincing  $V_2$  data below  $\sim 2$  GeV/c of transverse momentum ( $P_T$ ) [14, 17–19]. However, the hadronic rescattering effect on elliptic flow after the hadronization following by the hydrodynamics, at least in our knowledge, has not been investigated in details so far. In this paper, we shall focus on this effect. As a result, we find that  $v_2$  of final particles is suppressed due to the rescattering among hadrons to a considerable extent. It should be pointed out that the hadronic space before rescattering is produced directly through an anisotropic momentum space, which will be described in detail in the following.

For simplicity, the hydrodynamics [15, 16, 21, 22] that we are using assumes cylindrically symmetric transverse expansion with a longitudinal scaling flow profile ( $v_z = z/t$ ), though we want to investigate non-central collisions. We recognize that our initial phase space of hadrons in this way is not perfect, but it is still very useful and interesting since our main purpose is to research the effect of hadronic rescattering on elliptic flow. Initial conditions for Au+Au collisions at 200 GeV in 20–40% centrality are supposed that initial energy density = 10.3 GeV/fm<sup>3</sup>, initial time = 0.6 fm/c, and hydrodynamical evolution of cylindrically symmetric transverse expansion with a longitudinal scaling flow profile is adopted. When temperature of liquid reaches a point of critical energy density (= 0.42 GeV/fm<sup>3</sup>), a hadronization of QGP which is described by employing the MIT bag model EOS [12] will take place. And an ideal hadron gas is established and the corresponding EOS is applied. Hadronization in hydrodynamics usually obeys the rule of Cooper and Frye [13]. In this work, however, we make an assumption that the coordinate and momentum spaces of hadronized particles are not isotropic, but have elliptic shapes in order to simulate Au+Au collisions at 200 GeV in 20–40% centrality and get  $V_2$  in our calculation. Here, the mean anisotropy in momentum space,  $F = \langle P_x/P_y \rangle$ , takes 1.18 for all produced hadrons in our simulation.

For the details of the simulation to result in the above anisotropic distributions, we wrote:

$$\begin{aligned} R_x &= R_{T_x} \cos \theta & P_x &= P_{T_x} \cos \psi \\ R_y &= R_{T_y} \sin \theta & P_y &= P_{T_y} \sin \psi \\ R_z &= t * \tanh y & P_z &= m_T \sinh y \end{aligned}$$

$$(1) \quad T = \xi \tanh y \quad E = \sqrt{P_x^2 + P_y^2 + P_z^2 + m_0^2}$$

$$(2) \quad \langle P_{T_x}/P_{T_y} \rangle = \langle R_{T_y}/R_{T_x} \rangle = F$$

$$(3) \quad \langle \theta/\psi \rangle = 1$$

where  $m_T = \sqrt{p_T^2 + m_0^2}$ . ( $R_x, R_y, R_z, t$ ) and ( $P_x, P_y, P_z, E$ ) are the 4-vectors of produced hadrons in coordinate and momentum spaces, respectively. We assume that hadrons are randomly distributed in the overlap coordinate space of two spherical nucleus in terms of the Eq. (1) by hadronization. Here,  $\xi$  and  $y$  are random numbers distributed in  $\{0,14\}$  fm/c and  $\{-5,5\}$ , respectively. As for momentum and position of hadrons,  $P_{T_x}$  and  $R_{T_y}$  denote a random variable distributed in  $\{0,4\}$  GeV and  $\{0,7\}$  fm. After  $P_{T_x}$  and  $R_{T_y}$  sampling,  $P_{T_y}$  and  $R_{T_x}$  can be obtained by the anisotropic factor ( $F$ ) in momentum and coordinate space. The anisotropic factor ( $F$ ) makes our momentum and coordinate space distribution in transverse plane elliptic and anti-elliptic. If we make  $F$  equal to 1, our hadronization method will go back to the standard method of Cooper and Frye.  $\theta$  and  $\psi$  are the azimuths distributed in  $\{0,2\pi\}$  in coordinate and momentum spaces. But here we assume these produced hadrons are from a radial source in which  $\theta$  and  $\psi$  have a correlation like Eq. (3), which means once a  $\psi$  has been decided, the corresponding  $\theta$  will be selected in a gauss distribution whose mean is the  $\psi$  and whose width  $\sigma$  is always assumed to be 0.2 $\pi$

in our default calculation. Here, we choose the default anisotropic factor  $F$  in momentum space, equals to 1.18 for Au+Au collisions at 200 GeV in 20–40% centrality.

After the hadrons are produced, they enter next rescattering process among them. Here we use the rescattering model from LUCIAE [9, 11]. Two particles will collide if their minimum distance  $d_{\min}$  satisfies

$$(4) \quad d_{\min} \leq \sqrt{\frac{\sigma_{\text{total}}}{\pi}}$$

where  $\sigma_{\text{total}}$  is the total cross section in fm<sup>2</sup> and the minimum distance is calculated in the centre-of-mass frame of the two colliding particles. If these two particles are moving towards each other at the time when both of them are formed, the minimum distance is defined as the distance perpendicular to the momentum of both particles. If the two particles are moving back-to-back, the minimum distance is defined as the distance at the moment when both of them are formed. Assuming that the hadrons move along straight-line classical trajectories between two consecutive collisions, it is possible to calculate the collision time when two hadrons reach their minimum distance and order all the possible collision pairs according to the collision time sequence. If the total and the elastic cross section satisfies

$$(5) \quad \frac{\sigma_{\text{elastic}}}{\sigma_{\text{total}}} \geq \eta$$

where  $\eta$  is a random number, then the particles will be elastically scattered or else the collision will be considered as an inelastic reaction. The distribution of the momentum transfer,  $t$ , is taken as

$$(6) \quad \frac{d\sigma}{dt} \sim \exp(Bt)$$

where  $B$ , for an elastic scattering, depends on the masses of two scattering particles. The azimuthal angle will be isotropically distributed.

During the rescattering process, the following inelastic reactions are included in our calculation presented in Table 1, where the hyperons are  $Y = \Lambda$  or  $\Sigma$ .

**Table 1.** The inelastic reaction channels which are included in the hadronic rescattering model from LUCIAE, where the hyperons are  $Y = \Lambda$  or  $\Sigma$

$\pi N \Leftrightarrow \Delta N$	$\pi N \Leftrightarrow \rho N$
$NN \Leftrightarrow \Delta N$	$\pi\pi \Leftrightarrow k\bar{k}$
$\pi N \Leftrightarrow kY$	$\pi\bar{N} \Leftrightarrow \bar{k}\bar{Y}$
$\pi Y \Leftrightarrow k\Xi$	$\pi\bar{Y} \Leftrightarrow \bar{k}\bar{\Xi}$
$\bar{k}N \Leftrightarrow \pi Y$	$k\bar{N} \Leftrightarrow \pi\bar{Y}$
$\bar{k}Y \Leftrightarrow \pi\Xi$	$k\bar{Y} \Leftrightarrow \pi\bar{\Xi}$
$\bar{k}N \Leftrightarrow k\Xi$	$k\bar{N} \Leftrightarrow \bar{k}\bar{\Xi}$
$\pi\Xi \Leftrightarrow k\Omega^-$	$\pi X \Leftrightarrow \Omega^-$
$k\Xi \Leftrightarrow k\Omega^-$	$\bar{k}\Xi \Leftrightarrow \pi\Omega^-$
$\bar{N}N$ annihilation	$\bar{Y}N$ annihilation

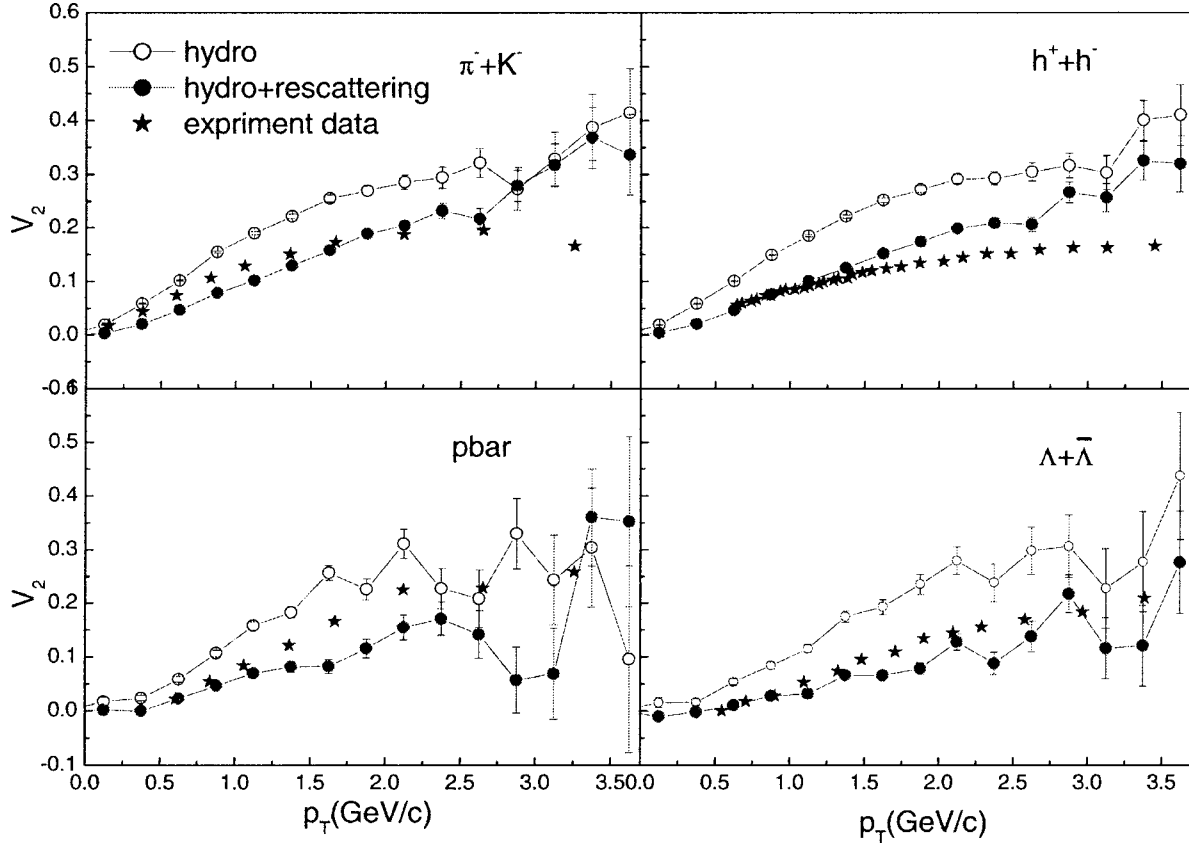


**Fig. 1.** The  $P_T$  dependences of  $V_2$  of  $\pi^- + \bar{k}$ ,  $h^- + h^+$ ,  $\bar{P}$  and  $\Lambda + \bar{\Lambda}$  before and after hadronic rescattering in hydrodynamics + rescattering model in 20–40% centrality Au+Au collisions at 200 GeV. The experimental data comes from [7] and [2].

The relative probabilities for the different channels, e.g. in  $(\pi N)$ -scattering, is used to determine the outcome of the inelastic encounter. As the reactions introduced above do not make up the full inelastic cross section, the remainder is again treated as elastic encounters.

We obtain the  $V_2$  of hadrons before and after rescattering in terms of formula (7), which indicates the anisotropy of hadrons momentum space.

$$(7) \quad V_2 \equiv \left\langle \frac{p_x^2 - p_y^2}{p_x^2 + p_y^2} \right\rangle$$

Figure 1 shows dependence of  $V_2$  of  $\pi^- + \bar{k}$ ,  $h^- + h^+$ ,  $\Lambda + \bar{\Lambda}$  on  $P_T$  before and after rescattering in hydrodynamics and experimental data in Au+Au collisions at 200 GeV in 20–40% centrality [8].

In order to research anisotropy of hadrons coordinate space, the parameter named as  $\varepsilon_2$  is defined by formula (8).

$$(8) \quad \varepsilon \equiv \left\langle \frac{x^2 - y^2}{x^2 + y^2} \right\rangle$$

The plots (a), (c) and (e) in Fig. 2 give  $P_T$  spectra,  $V_2$  and  $\varepsilon_2$  of four types of particles ( $(\pi^+ + \pi^-)$ ,  $(k^+ + k^-)$ ,  $(P + \bar{P})$ ,  $(\Lambda + \bar{\Lambda})$ ) as a function of  $P_T$  before and after rescattering in hydrodynamics + rescattering model. The open and full points respectively stand for the status before and after hadrons rescattering. We can see that

$P_T$  yield and  $\varepsilon_2$  of hadrons are enhanced by rescattering, and also note  $\varepsilon_2$  changes its sign through rescattering. On the other hand, elliptic flow  $V_2$  of hadrons is suppressed by the rescattering. In order to research the extent of the enhancement (or suppression) at different  $P_T$  bins, we define three factors named as  $s_{pT}$ ,  $s_{v_2}$  and  $D_{\varepsilon_2}$  by formulas (9), (10) and (11).

$$(9) \quad s_{pT} \equiv \frac{\frac{dN}{dy dP_{T\text{after}}}}{\frac{dN}{dy dP_{T\text{before}}}}$$

$$(10) \quad s_{v_2}(p_T) \equiv \frac{V_2(p_T)_{\text{after}}}{V_2(p_T)_{\text{before}}}$$

$$(11) \quad D_{\varepsilon_2}(p_T) \equiv \varepsilon_2(p_T)_{\text{after}} = \varepsilon_2(p_T)_{\text{before}}$$

The plots (b), (d) and (f) in Fig. 2 show respective  $P_T$  dependence of  $s_{pT}$ ,  $s_{v_2}$  and  $D_{\varepsilon_2}$ . In (b), we find that the yield of hadrons is increased by hadrons rescattering, especially for higher  $P_T$  yield. It indicates hadronic rescattering produces many secondary hadrons, whose  $P_T$  seems harder than those hadrons in last generation. In (d),  $s_{v_2}$  increases with  $P_T$ , which indicates the suppression effect on  $v_2$  from hadronic rescattering becomes weaker and weaker with increasing  $P_T$ . In (e) and (f), we see the rescattering turns the shape of

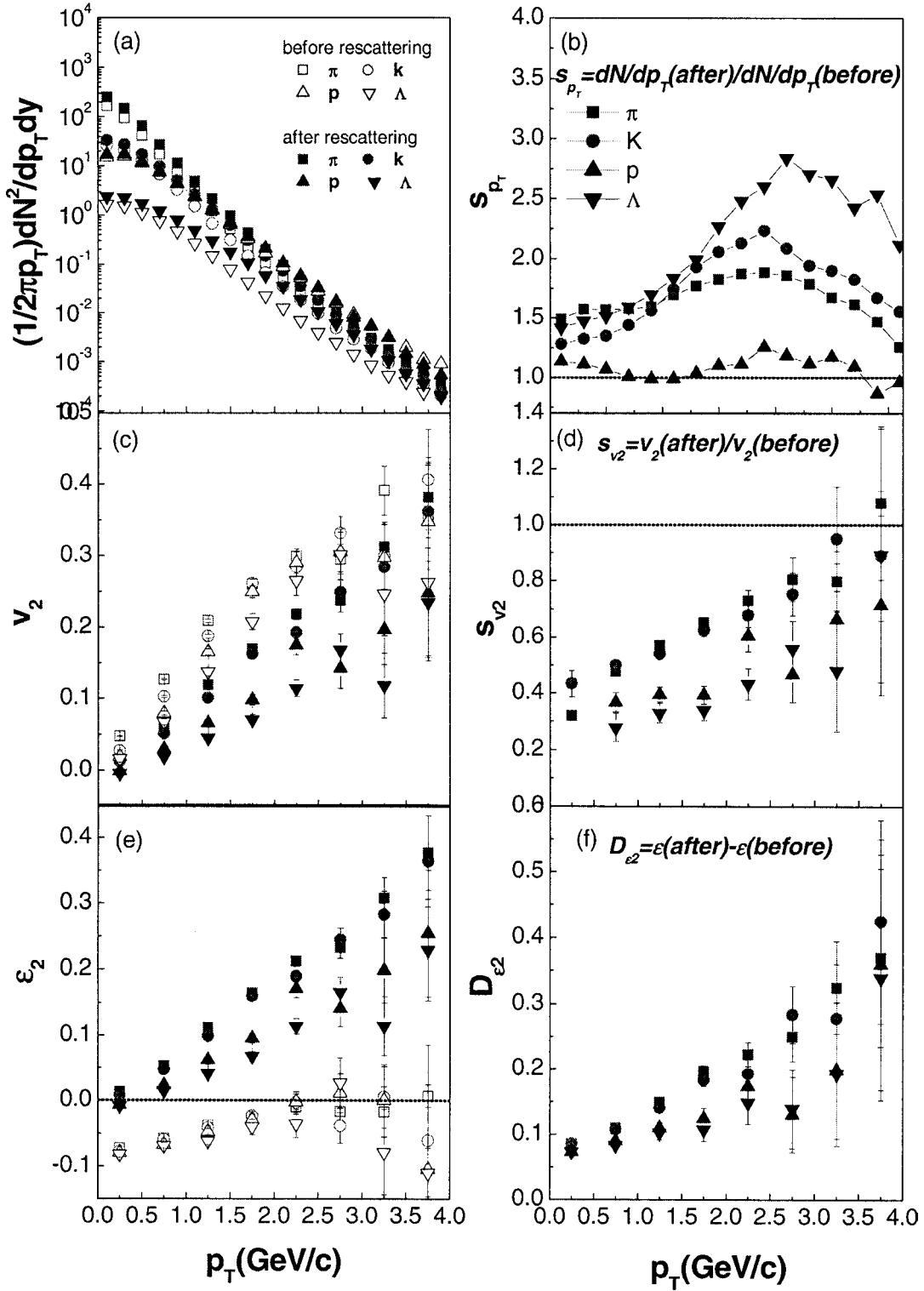


**Fig. 2.** Plot (a), (c), (e): the  $P_T$  dependences of spectra,  $V_2$  and  $\epsilon_2$  of  $\pi^+ + \pi^-$  (square),  $k^+ + k^-$  (circle),  $P + \bar{P}$  (up-triangle) and  $\Lambda + \bar{\Lambda}$  (down-triangle) before (open) and after (full) hadronic rescattering in hydrodynamics + rescattering model in 20–40% centrality Au+Au collisions at 200 GeV. Plot (b), (d), (f): the respective  $P_T$  dependences of  $s_{p_T}$ ,  $s_{v_2}$  and  $D_{\epsilon_2}$ .

coordinate space, and the effect become stronger with increasing  $P_T$ . It indicates the rescattering makes hadrons momentum space less anisotropy and more heavier particles, more suppression of the  $v_2$ . While the changes of the tropism of coordinate space occurs in the same time. In our calculation, at least 20 ~ 40%  $V_2$  will disappear through final hadronic rescattering.

Therefore, the effect from final hadronic rescattering on  $V_2$  maybe should be considered in order to research early state information in relativistic heavy-ion collisions.

In order to investigate the initial geometrical dependence of our results farther, we next attempt to take the Cooper-Frye hadronization method but with three different anisotropic conditions to see the change of

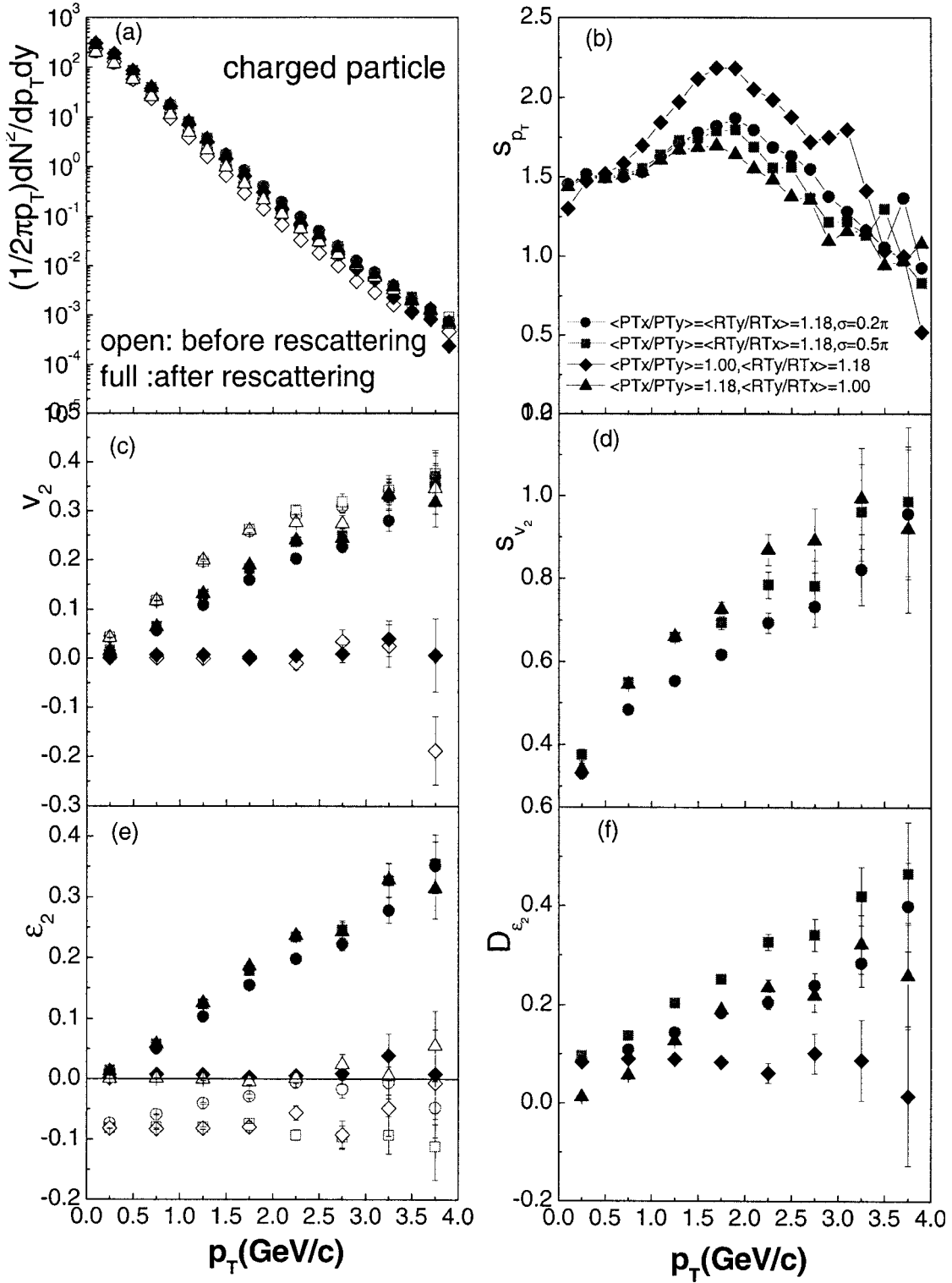


**Fig. 3.** Plot (a), (c), (e): the  $P_T$  dependences of spectra,  $V_2$  and  $\epsilon_2$  of charged particle before (open) and after (full) rescattering in hydrodynamical + rescattering model in 20–40% centrality Au+Au collisions at 200 GeV. The circles and squares both are for the hadronization with both initial  $v_2$  and  $\epsilon_2$ , and the circles correspond to  $0.2\pi$  of the width  $\sigma$  of  $\psi - \phi$  correlation and the squares correspond to  $0.5\pi$ . The diamonds are from the hadronization in which particles are with  $\epsilon_2$  and without  $v_2$ . The triangles are from the hadronization in which particles are with  $v_2$  and without  $\epsilon_2$ . Plot (b), (d), (f): the respective  $P_T$  dependences of  $s_{P_T}$ ,  $s_{V_2}$  and  $D_{\epsilon_2}$  in these four hadronization situations.

effect from final hadronic rescattering. Since the status of momentum and coordinate space before the hadronic rescattering cannot be measured by experiment, we assume another three conditions here.

- (i) We decrease the correlation between momentum space and coordinate space, i.e. increase  $\sigma = 0.2\pi$  into  $\sigma = 0.5\pi$ . As we see, the circles and squares in Fig. 3, the stronger correlation seem to produce

more hadrons and suppress  $v_2$  more strongly, but the change for the anisotropy of coordinate space  $\varepsilon_2$  is slight.

- (ii) The diamonds in Fig. 3 obviously shows that only hadronic rescattering cannot induce  $V_2$  if the interaction system has not anisotropy of momentum space before the hadronic rescattering, though its high  $s_{p_T}$  indicates that more secondary hadrons are produced in rescattering. On the other hand, the anisotropy of coordinate space also disappear after hadrons rescattering. It is also reasonable because the rescattering plays a role that it decreases  $V_2$  and tends to make the reaction system isotropic, which is consistent with the isotropic feature of rescattering angle in LUCIAE rescattering model. Therefore, the anisotropy of momentum space, i.e.  $V_2$ , may be produced in partonic state before hadronization if the hadronic rescattering has no direction-sense.
- (iii) We only remain anisotropy of momentum space, but lack of anisotropy of coordinate space when hadronization takes place as shown with the triangles in Fig. 3, the rescattering still decrease  $V_2$  of hadrons and produce a big anisotropy of coordinate space  $\varepsilon_2$ .

Not only in the above three conditions, but also in our default condition, we all find that hadronic rescattering produces many secondary hadrons and suppresses the elliptic flow  $V_2$  of hadrons to a certain extent. When the two kinds of anisotropies of coordinate and momentum space tend to be homologous with time, hadronic rescattering process ends and the reaction system freezes-out.

In conclusion, we apply a hydrodynamics + rescattering model to investigate the effect of hadronic rescattering on elliptic flow  $V_2$ . We find that hadron yield is increased after hadronic rescattering. The rescattering among the hadrons plays a suppression role for  $V_2$ , which makes the asymmetric system in momentum space into less anisotropic one. The suppression becomes weaker with increasing transverse momentum. We miss at least 20 ~ 40%  $V_2$  after hadronic rescattering in a hydrodynamics + rescattering model. Since the hadronic system created in RHIC collision is also very dense, the following hadronic rescattering may happen potentially and play an important role. Of course, only information on the momentum space after the freeze-out can be measured in experiment. But anyway, the effect of elliptic flow  $v_2$  from final hadronic rescattering deserves attention if the hadronization takes place when the energy reaches certain critical energy density in hydrodynamics.

**Acknowledgments** This work was supported partly by the Major State Basic Research Development Programme of China under Contract No. G200077400, the National Natural Science Foundation of China under Grant No. 10328259 and 10135030, and the Chinese Academy of Sciences Grant for the Distinguished Young Scholars of the National Natural Science Foundation of China under Grant No. 19725521.

## References

1. Ackermann KH *et al.* (STAR Collaboration) (2001) Elliptic flow in Au+Au collisions at  $\sqrt{s_{NN}} = 130$  GeV. *Phys Rev Lett* 86:402–407
2. Adams J *et al.* (STAR Collaboration) (2004) Particle-type dependence of azimuthal anisotropy and nuclear modification of particle production in Au+Au collisions at  $\sqrt{s_{NN}} = 200$  GeV. *Phys Rev Lett* 92:052302
3. Adcox K *et al.* (PHENIX Collaboration) (2002) Flow measurements via two particle azimuthal correlations at Au+Au collisions at  $\sqrt{s_{NN}} = 130$  GeV. *Phys Rev Lett* 89:212301
4. Adler C *et al.* (STAR Collaboration) (2001) Identified particle elliptic flow in Au+Au collisions at  $\sqrt{s_{NN}} = 130$  GeV. *Phys Rev Lett* 87:182301
5. Adler C *et al.* (STAR Collaboration) (2002) Azimuthal anisotropy of K0(S) and lambda + antilambda production at mid-rapidity from Au+Au collisions at  $\sqrt{s_{NN}} = 130$  GeV. *Phys Rev Lett* 89:132301
6. Adler C *et al.* (STAR Collaboration) (2003) Azimuthal anisotropy and correlations in the hard scatterin regime at RHIC. *Phys Rev Lett* 90:032301
7. Adler SS *et al.* (PHENIX Collaboration) (2003) Elliptic flow of identified hadrons an Au+Au collisions at  $\sqrt{s_{NN}} = 200$  GeV. *Phys Rev Lett* 91:182301
8. Adler SS *et al.* (PHENIX Collaboration) (2003) Identified charge particle spectra and yields in Au+Au collisions at  $\sqrt{s_{NN}} = 200$  GeV. *Phys Rev C* 69:034909
9. An T, Ben-Hao S (1999) J/Psi dynamic suppression in a hadron and string cascade model. *Phys Rev C* 59:2728–2733
10. Bass SA (2003) QGP theory: status and perspectives. *Pramana* 60:593–612
11. Ben-Hao S, Xiao-Rong W, An T *et al.* (1999) Enhancement of singly and multiply strangeness on p+Pb and Pb+Pb collisions at 158 AGeV/c. *Phys Rev C* 60:047901
12. Chodos A, Jaffe RL, Johnson K *et al.* (1974) A new extended model of hadrons. *Phys Rev D* 9:3471–3495
13. Cooper F, Frye G, Schonberg E (1975) Landau's hydrodynamic model of particle productions and electron positron annihilation into hadrons. *Phys Rev D* 11:192–213
14. Csanad M, Csorgo T, Lorstad T *et al.* (2004) Buda-Lund hydro model for ellipsoidally symmetric fireballs and the elliptic flow at RHIC. *Nucl Phys A* 742:80–94
15. Dumitru A, Bass SA, Bleicher M *et al.* (1999) Direct emission of multiple strange baryons in ultrarelativistic heavy ion collisions from the phase boundary. *Phys Lett B* 460:411–416
16. Dumitru A, Rischke DH (1999) Collective dynamics in highly relativistic heavy ion collisions. *Phys Rev C* 59:354–363
17. Hirano T (2001) In plane elliptic flow of resonance particles in relativistic heavy ion collision. *Phys Rev Lett* 86:2754–2757
18. Huovinen P, Kolb PF, Heinz U *et al.* (2001) Radial and elliptic flow at RHIC: furtherer predictions. *Phys Lett B* 503:58–64
19. Kolb PF (1999) Anisotropic flow from AGS to LHC energies. *Phys Lett B* 459:667–673
20. Reiter M, Dumitru A (1998) Entropy production in collisions of relativistic heavy ions: a signal for quark gluon plasma phase transition? *Nucl Phys A* 643:99–112
21. Rischke DH, Bernard S, Maruhn JA (1995) Relativistic hydrodynamics for heavy ion collisions. 1. General aspects and expansion into vacuum. *Nucl Phys A* 595:346–382

- 
22. Rischke DH, Pursun Y, Maruhn JA (1995) Relativistic hydrodynamics for heavy ion collisions. 2. Compression of nuclear matter and the phase transition of the quark-gluon plasma. Nucl Phys A 595:383–408
  23. Satz H (1984) Color screening in SU(N) gauge theory at finite temperature. Nucl Phys A 418:447c–465c
  24. Wilson KG (1974) Confinement of quarks. Phys Rev D 10:2445–2459